Unearthing the roots of degradation of *Quercus pyrenaica* coppices: a root-to-shoot imbalance caused by historical management?

Roberto Salomón[a], Jesús Rodríguez-Calcerrada[a], Elena Zafra[a], Cesar Morales-Molino[a,b], Aida Rodríguez-García[a], Inés González-Doncel[a], Jacek Oleksyn[c], Roma Zytkowiak[c], Rosana López[d], José Carlos Miranda[a], Luis Gil[a], María Valbuena-Carabaña[a]

[a] Forest Genetics and Ecophysiology Research Group, E.T.S. Forestry Engineering, Technical University of Madrid (UPM), 28040 Madrid, Spain

[b] Institute of Plant Sciences and Oeschger Centre for Climate Change Research, University of Bern, Altenbergrain 21, CH-3013, Bern, Switzerland

[c] Polish Academy of Sciences, Institute of Dendrology, Parkowa 5, PL-62-035 Kórnik, Poland

[d] Hawkesbury Institute for the Environment, University of Western Sydney, 2753 Richmond (NSW), Australia

Corresponding author: Luis Gil

Email: luis.gil@upm.es

Telephone: +34913367113

Fax: +34 913572293

Abstract

Slow growth, branch dieback and scarce acorn yield are visible symptoms of decay in abandoned *Quercus pyrenaica* coppices. A hypothetical root-to-shoot (R:S) imbalance provoked by historical coppicing is investigated as the underlying driver of stand degradation. After stem genotyping, 12 stems belonging to two clones covering 81 and 16 m^2 were harvested and excavated to measure above- and below-ground biomass and nonstructural carbohydrate (NSC) pools. To study root system functionality, root connections and root longevity were assessed by radiocarbon analysis. Seasonality of NSC was monitored on five additional clones. NSC pools, R:S biomass ratio and fine roots-to-foliage ratio were higher in the large clone, whose centennial root system, estimated to be 550 years old, maintained large amounts of sapwood (51.8%) for NSC storage. 248 root connections were observed within the large clone, whereas the small clone showed comparatively simpler root structure (26 connections). NSC concentrations were higher in spring (before bud burst) and autumn (before leaf fall), and lower in summer (after complete leaf expansion); they were always higher in roots than in stems or twigs. The persistence of massive and highly inter-connected root systems after coppicing may lead to increasing R:S biomass ratios and root NSC pools over time. We highlight the need of surveying belowground organs to understand aboveground dynamics of *Q. pyrenaica*, and suggest that enhanced belowground NSC storage and consumption reflect a trade-off between clonal vegetative resilience and aboveground performance.

Keywords

biomass partitioning, grafting, multi-stemmed tree, resprouting, forest decline, vegetative regeneration

Abbreviations

R:S, root-to-shoot ratio; NSC, non-structural carbohydrates; dbh, diameter at breast height; B_{ST}, stem biomass; B_{BR}, branch biomass; B_{FL}, foliage biomass; B_{CR}, coarse root biomass; B_{TP}, taproot biomass; B_{FR}, fine root biomass; DM, dry matter; DOY, day of year

1. Introduction

Quercus pyrenaica Willd. is a marcescent oak located in siliceous sub-Mediterranean regions from northern Morocco to south-western France, generally in montane slopes unsuitable for agriculture. *Q. pyrenaica* has been traditionally coppiced for firewood, charcoal and woody pastures. The vigorous root-resprouting ability of this species has determined its intense coppice use, consisting on short cutting cycles ranging from 7 to 15 years. Abandonment of historical coppicing in 1970s has revealed the current degradation state of most of stands, where overaged multi-stemmed trees present low stem growth, absent acorn yield, and high branch and stem dieback (Bravo et al., 2008; Cañellas et al., 2004). Several consequences of long-term coppicing are repeatedly suggested since the 1990´s as determinants of such decay: excessive stem density and acute competition among clonal stems, substrate oligotrophication, clonal carbon starvation, low genetic diversity, and disequilibrium between belowground and aboveground tree organs (Serrada *et al.*, 1992; Cañellas *et al.*, 2004; Corcuera *et al.*, 2006; Bravo *et al.*, 2008, and references therein). Although genetic diversity loss has been already discarded (Valbuena-Carabaña and Gil, 2013; Valbuena-Carabaña et al., 2008), actual causes of degradation remain unknown, and forest managers unsuccessfully try to convert coppices into high forests by thinning trials.

Belowground factors are rarely taken into account in ecology and forest management studies. Technical difficulties in surveying belowground attributes and delineating genotypes, unfeasible by naked-eye in this species, lead to disregard the effect of clones in aboveground stem performance. Yet, in a *Q. pyrenaica* coppice, clonal structure and root biomass have shown to have an effect on diametric stem growth (Salomón et al., 2013), and genetic analyses have revealed heterogeneous clonal structures and clones of up to 43 stems covering areas as large as 258.5 m^2 in some *Q. pyrenaica* stands (unpublished data). Since non-structural carbohydrate (NSC) allocation to storage organs can be actively regulated to cope with unfavorable conditions (Dietze et al., 2014; Sala et al., 2012), belowground influence on aboveground performance would partially come from a trade-off between carbon allocation to growth and

storage. Accordingly, enhanced NSC storage in roots is consistently displayed by resprouters to support vegetative regeneration after disturbance (e.g. Knox and Clarke, 2005; Paula and Ojeda, 2009; Zeppel et al., 2015; Zhu et al., 2012b), often at the cost of growth and sexual reproductive effort (Bond and Midgley, 2001; Clarke et al., 2013; Iwasa and Kubo, 1997; Poorter and Kitajima, 2007). Moreover, large amounts of living parenchyma needed to store NSC might entail high maintenance costs derived from root respiration processes. In this line, favored NSC allocation to roots may lead to high belowground maintenance costs and constrained aboveground performance, supporting the hypothesis of a root-to-shoot (R:S) imbalance as the main cause of tree decay in abandoned coppices of *Q. pyrenaica* (Corcuera et al., 2006; Salomón et al., 2013). Such imbalance would be higher in older and larger clones (Iwasa and Kubo, 1997) subjected to more coppicing events, which entail limitations to carbon gain (via foliage photosynthesis) but maintained carbon loss (via root respiration).

For experimental simplicity the relationship between resprouting ability, root traits and storage patterns has been predominantly studied in herbaceous and shrub species (see Clarke et al., 2010, and refences therein), as well as in young trees grown under controlled conditions (e.g. Knox and Clarke, 2005). However, given the laborious and costly task of excavating extensive soil areas, the study of root and carbon reserve dynamics in mature trees grown under natural conditions and subjected to actual disturbances remains largely unknown, as pointed out by Sala et al. (2012) and Clarke et al. (2010), and mostly limited to poplar trees (Ally et al., 2010; Jelínková et al., 2009). Quantification of the extent of root survival and, contrarily, root dieback and duraminization after aboveground disturbance (Tarroux et al., 2010) would help to evaluate R:S relationship in terms of living biomass. Likewise, assessing the longevity of parental roots supporting younger resprouts is necessary to evaluate stand decline and senescence, as well as individual tree resilience to frequent disturbances (Ally et al., 2010; de Witte and Stöcklin, 2010; Genet et al., 2010). Furthermore, whether original root connections persist and root grafting occurs to maintain clonal integrity or, oppositely, root disruption causes clonal

partitioning is of paramount importance to understand tree functioning and stand dynamics (Baret and DesRochers, 2011; Fraser et al., 2006).

In this work we study biomass, architecture and carbon storage capacity of the root system of *Q. pyrenaica* clonal trees in a coppice stand. The overarching goal is to shed light on a hypothetical R:S imbalance causing the generalized stagnation in growth and sexual reproduction of abandoned *Q. pyrenaica* coppices. We aim to answer several related questions: does the R:S ratio of multi-stemmed oak trees vary with clonal size? Is it similar to reported ratios of seed regenerated oaks? How NSC allocation patterns change seasonally, spatially and with clonal size? How old are belowground organs supporting vegetatively regenerated stems? Do multi-stemmed trees remain functionally connected through the roots? If so, to what extent roots remain functional after stem removal? An integrative approach was applied to answer these questions: (i) genetic analyses were performed to elucidate the clonal structure of an experimental plot; (ii) eight and four stems belonging to two different clones covering 100 m^2 were harvested and excavated to measure R:S ratios of total biomass, living woody biomass, NSC pools, as well as fine roots-to-foliage ratios; (iii) NSC seasonality was monitored on roots, stems and twigs in seven clones for a total of 24 stems; (iv) unearthed root systems were dissected and root connections were quantified; and finally, (v) root longevity was evaluated using radiocarbon dating.

2. Materials and Methods

2.1. Experimental site and clonal structure

The study took place in a monospecific *Q. pyrenaica* abandoned coppice located in the buffer zone of the National Park of "Sierra de Guadarrama" (Valsaín, Segovia, Spain), at an altitude of 1.140 m, in humic cambisol (40°52´ N latitude, 04°01´ W longitude). Mean annual temperature is 10.5 ºC and mean annual rainfall is 885 mm. The stand was subjected to coppicing since at least the 12th century for firewood, charcoal and woody pasture production until traditional management was neglected in 1970s (Manuel Valdés and Rojo y Alboreca, 1993); afterwards

two thinning events (J. Donés, personal communication) resulted in a regular even-aged coppice of 781 stems ha^{-1}.

Genetic analyses were performed to assess the clonal structure of one-hectare experimental plot (see Salomón et al. 2013 for detailed information). Twelve stems from two clones of contrasted size were harvested and excavated for biomass partitioning. The larger clone covered 81 m^2 and was composed by eight stems (12 taking into account four stems felled in 2008 for other purposes) whereas the smaller clone was composed by four stems covering 16 m^2 (see Table 1 for aboveground features of the sampled stems). Clonal surface was estimated from polygons enclosing stems with the same genotype and adding an outer conservative buffer of 1.5 m using ArcGIS 10.1 software.

2.2. Aboveground biomass

The 12 stems were harvested in 2013 before leaf fall, from DOY 280 to 282. Diameter at breast height (dbh), stem height, and height of the life crown were measured after felling. Stem disk samples were taken at the stem base, breast height, 3 m height, and every two meters from this point. To quantify the contribution of the functional wood containing living parenchyma (sapwood) to total stem biomass, the depth of the different tissues (heartwood, sapwood and bark) were measured on four perpendicular radii at every disk sample, and three coaxial cylinders were assumed for cubication using Newton equation. Densities (dry matter [DM]/fresh volume, g cm^{-3}) were estimated per stem and tissue (heartwood, sapwood and bark) in subsamples from the 5 m-disk; they were cubicated by the Archimedes principle and weighted to the nearest 0.1 mg (Adventurer precision balance, Ohaus Corporation, NJ, USA) after 48 h at 65 ºC. Stem biomass (B_{ST}, kg of DM) was partitioned into heartwood, sapwood and bark after calculating the corresponding products of volume and density. Branch fresh biomass was weighted *in situ* to the nearest 20 g (BMM-BR80, Baxtran, Spain), and branch dry biomass (B_{BR}, kg DM) was calculated from fresh weight measurements minus the average relative water content registered in the stem disk samples. The proportion of heartwood, sapwood and bark in

148 branches was estimated as a function of their radii (Appendix A). Three branches per stem
149 (from the lower, middle and upper crown position) were defoliated and dry foliage biomass
150 (B_{FL}, kg DM) per branch was weighted. B_{FL} in non-defoliated branches was calculated as a
151 function of B_{BR} ($B_{FL} = 0.044 + 0.102 \times B_{BR}$, $P < 0.001$, $R^2 = 0.876$).

152 **2.3. Belowground biomass**

153 Prior to excavation, soil trenches of 1.5 m depth and width were dig downstream with a backhoe
154 to facilitate water and soil evacuation. Root systems were hydraulically excavated up to 1 m
155 depth using water sprays, high pressure water pumps, and tankers of the National Park
156 firefighters to load water from the nearest water source (the Eresma river, 3 km away from the
157 plot). Once unearthed, root systems were extracted with a backhoe. Biomass of coarse roots and
158 taproots (B_{CR} and B_{TR}, kg DM) was estimated from fresh weight measurements minus the
159 average relative water content of ten sampled roots, subsampled every meter for an overall of 39
160 root disk samples. The biomass of non-weighted coarse roots growing beyond the excavated
161 area was calculated as a function of the root diameter (mm) at its distal end ($biomass = 0.0094 \times$
162 $diameter^{1.4571}$, $n = 39$, $P < 0.001$, obtained from the sampled disks). The proportion of
163 heartwood, sapwood and bark within coarse roots was estimated from the average relative
164 volume observed in the root disks, as calculated for stems given the regular cylindrical shape of
165 coarse roots. Taproots (including the stump and the straight tapering root) were classified in
166 three groups: young taproots of trees felled in 2013, young taproots of trees felled in 2008, and
167 old taproots from previous unrecorded cutting events visible after excavation. The proportion of
168 heartwood, sapwood and bark within taproots was estimated by two different approaches
169 depending on the taproot shape and its degree of degradation. First, non-degraded taproots with
170 regular cylindrical-conical shapes ($n = 25$) were axially cut in four wedges. Radii of different
171 tissues were measured horizontally at different taproot depths every 3.5 cm. Coaxial and
172 superimposed cylinders of revolution were assumed for cubication. Second, degraded taproots
173 of irregular shape ($n = 20$) were cut across the plane with largest surface. Surfaces of different
174 tissues were measured on both sides with a mechanical planimeter (Haff, No. 317E, Germany)

and spherical shapes were assumed for cubication. Since hydraulic excavation lead to fine roots loss, soil cores were previously sampled with a soil borer to estimate fine roots abundance at six locations per clone and two depths (0-30 and 30-60 cm). Soil cores were carefully washed to remove soil and stones. Fine roots were classified into small fine roots (diameter < 2 mm) and large fine roots (diameter = 2-5 mm), and then dried and weighted (Barbaroux et al., 2003; Vanninen and Makela, 1999). Densities of small fine roots and large fine roots were estimated on a soil volume basis (g dm^{-3}). To assess fine root biomass lost during excavation, fine root density (B_{FR}, g dm^{-3}, considering both small and large fine roots) was extrapolated to the soil volume surveyed per clone (81 and 16 m^2 by 0.6 m depth). Note that coarse and taproots were excavated up to 1 m depth, whereas fine roots were sampled up to 0.6 m due to difficulties in coring beyond this soil depth.

2.4. Total non-structural carbohydrates

Twigs, stems and roots were sampled for NSC determination in the 12 harvested stems. Samples were collected in one year-old twigs, at stem breast height, and in coarse roots located 50-100 cm away from the stem base. NSC sampling took place during 2013 at three phenological stages: before budburst (DOY 99, April), after complete leaf expansion (DOY 170, June), and at the end of the growing season, before leaf fall (DOY 275, October). Additionally, 12 stems belonging to five extra clones of contrasted sizes (two large clones > 45 m^2, and three small clones < 20 m^2) were sampled in June and October, during the expected lowest and highest NSC concentrations, respectively (Barbaroux et al., 2003). After collection, samples were frozen in liquid nitrogen for transportation to the laboratory and stored at -80 °C until lyophilization. Total NSC was determined on sapwood as described by Oleksyn et al. (2000) as the sum of soluble sugars and starch concentrations. Soluble sugars were extracted from oven-dried (65 °C, 48 h) tissue powdered in methanol:chloroform:water solution (12:5:3 by volume), and the residue was used for starch determination. Soluble sugar concentration was measured colorimetrically in a spectrophotometer at 625 nm wavelength within 30 minutes, following a color reaction with anthrone reagent. Starch was converted to glucose with

amyloglucosidase and further oxidized using the peroxidase-glucose oxidase complex; its concentration was measured at 450 nm, following the reaction with dianisidine. [NSC] was expressed on a dry matter basis (%).

2.5. Root structure and connections

Once excavated, the root system architecture was analyzed *in situ* before root extraction and in the laboratory. Root connections were classified into two categories: (i) parental roots from which stems resprouted and (ii) root grafts occurring after stem resprouting (DesRochers and Lieffers, 2001a). Root grafts were confirmed after bark removal to assess common annual tree rings between roots. In the large clone, a string grid of 0.5 m by 0.5 m was arranged above the soil level to photograph in detail the root system. A total of 269 photographs were bound with Photoshop software to obtain a picture of the whole root system where every taproot and root connection was identified by its corresponding label and depicted using Adobe Illustrator. The small clone was photographed without any grid. To quantify graft size, the smallest root within the graft was considered and its cross (connecting) section was estimated from two perpendicular diameters at each graft side. To estimate cross connecting section of parental roots, their average diameter was measured at the midpoint between connected taproots. Cumulative connecting section per clone (the sum of connecting sections) was estimated for grafts and parental roots. Cumulative sapwood connecting section was estimated from the relationship between root radius and its relative sapwood section (Appendix A).

2.6. Root radiocarbon dating

With the purpose of dating the age of the trees, we targeted the apparently oldest roots within the clones for radiocarbon dating. Three taproots from the large clone and one taproot from the small clone were chosen. For radiocarbon analysis, α-cellulose was extracted using a modification of the James-Wise protocol (Capano et al., 2010), because its low mobility in wood make it suitable for annual ^{14}C signatures (Tandoh et al., 2013). We took a subsample of wood from the innermost part of each taproot cross section because the oldest wood is expected

to be in that position. Wood subsamples for ^{14}C dating spanned the lowest possible number of tree rings to better constrain the age, and were carefully cleaned to avoid contamination with modern carbon. Analyses were performed at the Center for Isotopic Research on the Cultural and Environmental Heritage (CIRCE, Naples, Italy). Measured ^{14}C ages were converted into calendar years using the program CALIBomb (Reimer and Reimer, 2004) coupled with the INTCAL13 calibration curve (Reimer et al., 2013) and the Northern Hemisphere Zone 1 compilation for radiocarbon dates younger than 1950 AD (Hua et al., 2013).

2.7. Statistical analyses

To estimate R:S ratios, aboveground biomass (B_{ST}, B_{BR} and B_{FL}) was first estimated individually per stem and then summed per clone, whereas belowground biomass (B_{TR}, B_{CR} and B_{FR}) was directly estimated per clone. Differences in fine root density between clones and soil depths were assessed with linear models using R software (version 3.1.1). For non-linear regressions (as for weight-diameter relationships), *nls* function in the stats library was used. To study variability in NSC, soluble sugars and starch concentrations, hierarchical mixed models were performed using the *lme* function in the nlme library, in which sampling date, organ, clonal size, and their interactions were treated as fixed factors whereas stem (n = 24) nested within its corresponding clone (n = 7) was treated as a random factor. Backward selection was used to select the most appropriate model until all variables were significant at $\alpha = 0.05$. Multiple comparisons on the [NSC] among sampling dates and tree organs were performed with the *glht* function in the multcomp library. NSC pools in stems and branches (kg) were calculated per stem as the product of their corresponding sapwood biomass by their average [NSC] across sampling dates. Belowground NSC pool was calculated per clone as the product of average root [NSC] across sampling dates and root sapwood biomass. All values presented in the text are means and standard errors.

3. Results

3.1. Aboveground and belowground biomass

254 Average stem dbh and number of annual growth rings (as an estimator of stem age) were 18.6
255 (1.0) cm and 45.8 (0.7) (Table 1), and similar between clones (P = 0.377 and P = 0.870,
256 respectively). Pooling data from the large and small clones, the relative contribution of leaves,
257 branches and stems to the total aboveground biomass was 3.2, 28.6 and 68.2%, respectively
258 (Figure 1a, Table 1). Heartwood, sapwood and bark densities were 0.72 (0.01), 0.61 (0.01) and
259 0.50 (0.01) g cm^{-3}, respectively. The contribution of heartwood, sapwood and bark to the
260 aboveground woody biomass (B_{ST} and B_{BR}) was 27.5, 46.5 and 26.0%, respectively (Figure 1b,
261 Table 1). Overall, aboveground biomass in the large clone was 2.5 times that of the small clone
262 (1450.5 and 588.6 kg, respectively).

263 Pooling data from the large and small clones, fine roots, coarse roots and taproots accounted for
264 8.7, 62.7 and 28.6%, respectively, of the belowground biomass (Figure 1a, Table 2). The
265 contribution of heartwood, sapwood and bark to the belowground woody biomass (B_{CR} and B_{TR})
266 was 23.0, 52.1 and 24.9%, respectively. Taproots maintained relatively large amounts of
267 functional biomass after stem felling: although the proportion of heartwood was higher in old
268 taproots than in young taproots to the detriment of sapwood, the reduction in the relative
269 sapwood volume was limited to 14.2% (i.e., from 53.3 to 39.1%, Figure 2). Small fine roots
270 accounted for the greatest portion of fine roots (87.7 and 12.3% for small and large fine roots,
271 respectively, Table 2). Density of fine roots tended to be greater in the large clone (P = 0.061),
272 and was constant between soil depths (P = 0.294). Estimates of B_{FR} were 124.4 and 24.6 kg for
273 the large and the small clones, respectively. Overall, belowground biomass in the large clone
274 was 4.4 times that of the small clone (1390.2 and 315.3 kg, respectively).

275 Root-to-shoot ratios of total biomass, woody biomass (excluding B_{FL} and B_{FR}), sapwood
276 biomass, and fine roots-to-foliage were consistently higher in the large clone (Figure 3).

277 **3.2. Total non-structural carbohydrates**

278 Pooling tree organs (roots, stems and twigs), average [NSC] at April, June and October was
279 13.2 (1.4), 6.7 (1.1) and 14.3 (1.1) %, respectively. Similar temporal fluctuations were observed

for roots and stems separately: [NSC] dropped to minimum values after leaf expansion (June) and increased after the growing season (October) to values similar to those observed prior to budburst (April, Figure 4). A similar temporal trend was found for twigs, although differences in [NSC] between April and June were marginally significant ($P = 0.063$). Vertical variations among organs were also observed: [NSC] in April increased downward from twigs to roots; whereas in June and October, differences were uniquely observed between below- and aboveground organs (Figure 4). Pooling sampling dates, average [NSC] for roots, stems and twigs was 15.4 (1.1), 8.9 (1.1) and 7.9 (1.1) %, respectively. Multiple comparisons showed that seasonal and vertical variability in [NSC] was mainly driven by fluctuations in starch concentrations (Figure 4). Differences in [NSC] between the large and small clone were uniquely observed before budburst in roots ($P = 0.002$, Figure 5), also due to differences in starch concentrations ($P = 0.004$). Higher root [NSC] and biomass in the large than in the small clone led to much higher NSC pools in the former (Figure 1c), and to R:S ratios for NSC pools >1 in the large clone (Figure 3).

3.3. Root structure, connections and age

A shallow root system was observed in both clones, with most coarse roots growing horizontally within a soil layer of one meter depth, and rare vertical roots growing below. Within the large clone, 74 taproots were counted; twelve taproots corresponded to harvested stems on 2013 and 2008; the remaining 62 old taproots showed high heterogeneity in size, shape and degradation state. Taproots were connected by a total of 248 root connections: 189 root grafts and 59 parental roots (Table 3, Figure 6b). Of the 189 root grafts, 73 (39%) connected young taproots, 70 (37%) connected young to old taproots, and 46 (24%) connected old taproots. Of the 59 parental connections, 6 (10%) connected young taproots, 29 (49%) connected young to old taproots, and 24 (41%) connected old taproots. The root system of the smaller clone was comparatively simpler: it was composed by four young taproots and two old taproots connected by 20 grafts and 6 parental roots. In both clones, although parental root connections were less frequent than root grafts, they were larger in size, resulting in greater

cumulative connecting section (Table 3). Very large size of two parental roots in the small clone substantially reduced differences in the sapwood-connecting section between the large and small clones.

The results of the radiocarbon dates are summarized in Table 4. The main finding is that the oldest taproot of the large clone was at least nearly 400 years old (1631 AD) if we consider the most conservative scenario. The period from 1397 to 1523 AD (roughly 500-600 years ago) is the likeliest for the formation of this root (Table 4, Figure 7), and the median of the probability distribution of the age is 1450 AD, thus over 550 years old. The other two dated taproots from the large clone were younger, with the likeliest age being around 80-200 years, and possibly even younger for one of the roots (50-60 years). Median ages for these taproots are ca. 150 years (1850-1860 AD). The small clone was younger than the large one and its age most likely lies within the intervals 1644-1694 and 1726-1813 AD, roughly speaking 200-370 years old, although we cannot discard it is only 60-80 years old. The median age is around 240 years (1770 AD).

4. Discussion

4.1. High root-to-shoot ratios in centennial coppiced trees

R:S biomass ratios in a large and a small clone of *Q. pyrenaica* (0.96 and 0.54, respectively) were higher than those previously reported for this species (0.30-0.35 in Montero *et al.*, 2005 and Ruiz-Peinado *et al.*, 2012) and other *Quercus* tree species (0.25 for *Q. petraea* in Barbaroux *et al.*, 2003; 0.36 for *Q. douglasii* in Millikin *et al.*, 1997; and 0.28 to 0.52 for seven species of Iberian *Quercus* in Montero *et al.*, 2005; Ruiz-Peinado *et al.*, 2012). Similarly, lower mean R:S biomass ratios have been reported across major terrestrial biomes: 0.30 in temperate oak forests (Mokany et al., 2006), 0.25 for angiosperms (Cairns et al., 1997), and 0.27 in temperate forests (Poorter et al., 2012). One reason for the higher R:S biomass ratios in our study is the consideration of the clonal structure of the tree, since trees are commonly considered as discrete units (originated from seeds) in most R:S reports. We suspect that R:S ratios of resprouting

333 species are systematically underestimated when neglecting their clonal structure due to the large
334 amount of non-sampled roots (Poorter et al., 2012; Robinson, 2004). For instance, if uniquely
335 taproots and crown roots initially extracted by pulling the stumps were considered for root
336 biomass (as in Montero *et al.*, 2005), the average R:S ratio for the 12 surveyed stems would
337 have been lower (0.44). Accordingly, mean R:S ratios of other clonal *Quercus* tree species was
338 high when the whole root system of multi-stemmed trees was excavated: 1.2 and 0.91 for *Q. ilex*
339 (Canadell and Roda, 1991; Serrada Hierro et al., 2013; respectively), 3.5 for *Q. coccifera*
340 (Cañellas and San Miguel, 2000), and 2.2 for *Q. aquifolioides* (Zhu et al., 2012b). Another
341 reason explaining high ratios of these studies and of *Q. pyrenaica* here is the resprouting nature
342 of the species. Resprouters allocate more biomass into roots than seeders under similar growing
343 conditions (Bond and Midgley, 2001; Clarke et al., 2013), leading to mean R:S ratios of 0.64
344 and 0.30, respectively (see meta-analysis of Poorter *et al.*, 2012, ratios inferred from the root
345 mass fraction), or even higher in the case of *Populus tremuloides* (from 0.46 to 3.42;
346 DesRochers and Lieffers, 2001b). The exponential decrease of the R:S ratio with stand age
347 reported in a compilation of 31 studies on *Quercus* species (Genet et al., 2010) yielded a R:S
348 ratio of 0.28 for the age of the stems studied here (46 years). This predicted value is lower than
349 the ones we observed (0.96 and 0.54) thus denoting root systems proportionally larger in
350 comparison to coetaneous stems of sexual origin. Furthermore, the R:S ratio was higher in the
351 larger clone, suggesting massive root development in old clones (Figures 6, 7) subjected to
352 more coppicing events. In support of this pattern, increasing clonal size in *Q. ilex* resulted in
353 higher R:S ratios, ranging from 0.23 in a single-stemmed tree to 1.92 in a seven-stemmed tree,
354 with intermediate ratios of 0.86 and 0.84 in three- and four-stemmed trees (Canadell and Roda,
355 1991). Similarly, Serrada *et al.* (2013) also observed progressive increment of R:S ratios from
356 0.69 to 0.99 with increasing number of stems within clones of *Q. ilex*. In any case, the costly
357 and laborious work required to excavate large trees vegetatively regenerated from root suckers
358 limited this study to two multi-stemmed individuals (entailing 100 m^2 excavations); therefore,
359 any extrapolation should be taken with caution.

Since woody biomass accounted for most of tree biomass (94.3%), R:S ratios of woody biomass were similar to those of total biomass. Moreover, due to the larger contribution of sapwood to belowground woody biomass (52.1 and 46.5% for below- and above-ground woody biomass, respectively), R:S ratios of sapwood increased up to 1.00 and 0.59 for the large and small clone, respectively (Figure 3). Consistently, the sapwood volume of old taproots compared to young taproots only decreased by 14% over time (Figure 2), pointing to high maintenance costs of living tissues belowground to cope with disturbances aboveground and maintain integral functionality of root-connected stems, as previously observed in clonal poplar trees (DesRochers and Lieffers, 2001a; Jelínková et al., 2009) and grafted pine trees (Tarroux et al., 2010). The persistence of massive parental root systems is consistent with the greater amount of fine roots in the larger clone. Since leaf biomass per stem was similar between clones ($P = 0.572$, Table 1), greater soil volume (containing fine roots) per stem in the larger clone resulted in higher fine roots-to-foliage ratio compared to the smaller clone: 2.69 and 1.28, respectively (Figure 3). These values are above the reported range – up to 1.25 for conifer species (e.g. Helmisaari et al., 2007; Vanninen and Makela, 1999), 0.39 and 0.36 for oak and beech, respectively (Barbaroux et al., 2003) – denoting relatively high metabolic activity belowground in the individuals of *Q. pyrenaica*. The fine roots-to-foliage ratio plays a pivotal role in tree water and carbon fluxes (Mokany et al., 2006; Vanninen and Makela, 1999), despite the low contribution of fine roots and foliage to total biomass in adult trees (5.7 % in this study). Higher leaf water supply and carbon uptake would be expected in the larger clone because of the greater amount of fine root biomass per leaf biomass. However, under conditions of restricted soil water content and photosynthesis, allometric differences could lead to physiological disequilibrium between the carbon source and sinks. Accordingly, increasing root respiration rates per stem in larger clones (Salomón et al., 2015) may be partially explained by great amounts of fine roots (metabolically more active than woody roots).

High maintenance of sapwood in woody roots of old root systems also implies high NSC storage capacity (Figure 1). This is consistent with high starch partitioning in roots relative to

387 above-ground organs (Figure 4), and with literature of resprouting species regenerating from
388 stumps or roots (e.g. Knox and Clarke, 2005; Paula and Ojeda, 2009; Zeppel et al., 2015; Zhu et
389 al., 2012b). Starch is mainly stored in parenchyma rays (see Clarke et al. 2013 and references
390 therein), as denoted by the positive relationship between [starch] and size of parenchyma across
391 several species of Ericaceae (Bell and Ojeda, 1999; Bell et al., 1996), Fagaceae and Rosaceae
392 (Rodríguez-Calcerrada et al., 2015). This positive linear relationship holds within *Q. pyrenaica*
393 trees (data reanalyzed from Rodríguez-Calcerrada et al., 2015), suggesting that the size of the
394 NSC pool is determined by the quantity of living cells and that the maximum [NSC] per living
395 cell is rather constant. Anatomical observations of the surveyed roots confirmed the large width
396 of root parenchyma rays, which were up to 40 cells wide (Appendix B).

397 Seasonal fluctuations of [NSC] reached lowest values after leaf expansion (June) and maximum
398 values before leaf fall (October) and at end of the dormancy period (April) (Figures 4 and 5), as
399 similarly observed in *Q. petraea* and *Q. aquifolioides* (Barbaroux and Bréda, 2002; Zhu et al.,
400 2012a). This result evidences the use of NSC reserves in satisfying spring demand for leaf
401 production and stem growth. NSC reserves during the dormant period favor tree resilience
402 under unfavorable conditions (Li et al., 2008; Zhu et al., 2012a). Here, differences in
403 belowground [NSC] between clones were observed before budburst (Figure 5), suggesting as in
404 other resprouting species an increasing resilience with clonal size and/or age (Clarke et al.,
405 2013; Jelínková et al., 2009; Tanentzap et al., 2012). Such higher resilience to aboveground
406 perturbations may come at the cost of growth (Bond and Midgley, 2001; Clarke et al., 2013;
407 Poorter and Kitajima, 2007; Sala et al., 2012) and lead to high ratios of "storage to production"
408 in long-lived larger individuals (Iwasa and Kubo, 1997), as here denoted by the high R:S ratios
409 of NSC pools (Figure 3). In a review on carbon allocation patterns, Sala *et al.* (2012) noticed the
410 scarcity of data on the stored NSC per unit of living biomass with plant size due to the difficulty
411 to quantify total NSC pools and living biomass on large individuals. Here, we observe high
412 belowground [NSC] and R:S ratios of NSC pools in large and old clones, and we report a
413 remarkable belowground NSC pool for a single tree (87.2 kg).

414 **4.2. High interconnection among roots in centennial coppiced trees**

415 Contrary to the expectation of root disruption causing clonal partitioning and stem
416 individualization as clonal trees grow (Bravo *et al.*, 2008, and references therein), a high
417 number of root connections was observed for both clones (248 and 26 for the large and the
418 small clone, respectively). The number of root connections on a surface basis was greater in the
419 larger and older clone (3.1 connections m^{-2}) than in the smaller clone (1.6 connections m^{-2}),
420 reinforcing the hypothesis of increasing degree of interdependence over time (DesRochers and
421 Lieffers, 2001a; Jelínková et al., 2009). Comparison with scarce literature reveals that root
422 grafting in *Q. pyrenaica* (Table 3) was much more frequent than in other species: e.g. 0.5 grafts
423 $stem^{-1}$ in *Populus tremuloides* (Jelínková et al., 2009), and 0.3 to 0.9 grafts $tree^{-1}$ in *Pinus*
424 *banksiana* (Tarroux and DesRochers, 2011; Tarroux et al., 2010). Moreover, we suspect that the
425 degree of clonal intra-connection in *Q. pyrenaica* is actually higher, considering missed
426 connections beyond the excavated area, and the difficulty to find root grafts below 30-40 cm
427 depth within these tangled systems. Furthermore, since root graft frequency depends on stem
428 physical proximity rather than genetic proximity (Tarroux et al., 2014), we also suspect the
429 occurrence of inter-clonal grafts that would result in larger functional individuals integrated by
430 different genotypes. Larger excavations in *Q. pyrenaica* coppices, that usually reach extremely
431 high stem densities, would confirm this hypothesis. The importance of root grafting for tree
432 performance is evidenced by NSC sharing within trees to support growth of suppressed stems
433 (Fraser et al., 2006) and even roots of removed stems (Tarroux et al., 2010). Since NSC transfer
434 among stems is dependent on the size of the root connection (Fraser et al., 2006), it is worth to
435 note that, within clones, the cumulative connecting area among roots (11.5 and 7.3 dm^2 for the
436 large and the small clone, respectively; Table 3) was 25% higher than the cumulative basal area
437 at breast height (considering uniquely functional sapwood area). Frequent root connections and
438 large connection sizes may explain higher homogeneity in [NSC] among stems within the same
439 clone (standard deviation = 0.78) than among the seven monitored clones (standard deviation =
440 2.54). Moreover, physiological interactions among stems in water and carbon fluxes may occur

441 through root connections (see Baret & DesRochers, 2011) and are suggested here by the
442 positive relationship between the cumulative root connecting area per stem and [CO_2] at the
443 base of the stem (as an indicator of root respiration activity, in prep.). Cooperative functioning
444 among connected stems may contribute to tree colonization and space occupation, and so to tree
445 persistence and competition (Bond and Midgley, 2001; Tanentzap et al., 2012; Tarroux and
446 DesRochers, 2011), a strategy that might govern dynamics in *Q. pyrenaica* stands. Knowledge
447 of the longevity of clonal species is crucial to understand population dynamics and interpret R:S
448 ratios. However, age assessment is not straightforward in these species, since ages of above- and
449 below-ground organs are decoupled (de Witte and Stöcklin, 2010). Accordingly, clonal size is
450 commonly suggested as a proxy of age because of the radial vegetative spread of long-lived
451 clonal plants (de Witte and Stöcklin, 2010; but see Ally et al., 2010). Our radiocarbon dates
452 suggest an older origin for the more complex and more inter-connected large clone (Table 4,
453 Figure 7). However, these dates should be considered as minimum estimates of the actual age of
454 *Q. pyrenaica* individuals. For an accurate date, the taproot developed from the original acorn
455 should be identified and sampled (if it still persists), an extremely difficult task given the
456 uncertain life history of clones and the unknown expansion mode of roots. Three radiocarbon
457 samples in the large clone did probably not capture the whole life history of this individual, and
458 greater sampling intensity would have helped to find other roots older than 550 years. In any
459 case, the old age observed for the large clone shows that *Q. pyrenaica* maintains its resprouting
460 ability for at least 400-500 years, thus much longer than previous speculations around 200
461 (Ximénez de Embún, 1961) or 300 years (Bravo *et al.*, 2008, and references therein).

462 Vegetative regeneration predominates in certain resprouting species to the detriment of sexual
463 regeneration, particularly in Mediterranean ecosystems subjected to frequent disturbances (Bond
464 and Midgley, 2001). In the case of *Q. pyrenaica*, regeneration dynamics is determined to a great
465 extent by vegetative resprouting induced by anthropogenic perturbations (Camisón et al., 2015;
466 Valbuena-Carabaña and Gil, 2013), as is the case in this experimental plot where the
467 contribution of clonal regeneration is above 80% (Salomón et al., 2013). Palynological research

conducted on sediments from a mire close to the study plot shows a marked decline in the concentration of pollen from deciduous *Quercus* ca. 400 years ago (Appendix C). This important drop could be linked to decreased pollen productivity as a consequence of the shift from sexual to vegetative regeneration by conversion to coppice systems. Historical sources support this interpretation, as the general establishment of leasing contracts for forest use in the early modern period (Manuel Valdés and Rojo y Alboreca, 1993) would have intensified oak wood exploitation, and promoted vegetative regeneration (every 7-15 years) in detriment of pollen yield. We conclude that symptoms of poor aboveground performance in overaged stems, commonly interpreted as clonal decay may instead suggest strong vegetative resilience. In this framework, current attempts of conversion of *Q. pyrenaica* coppices into high forests by thinning would be hindered by the progressive increase in R:S ratios, despite transient increases in growth of residual stems (Bravo et al., 2008; Cañellas et al., 2004; Corcuera et al., 2006).

5. Conclusions

Survey of hidden tree organs is essential to understand the performance of above-ground organs. Here, an integral view of the whole tree – including belowground roots – has been conducted to explain the poor performance of *Q. pyrenaica* above ground after the abandonment of traditional coppicing. We have observed that periodical and sustained coppicing lead to massive root systems with large amounts of living biomass and root NSC pools that ensure persistence by resprouting after above ground perturbations, but that can contribute to "stand decline" by exacerbating root carbon costs through respiration. Moreover, the promotion of vegetative regeneration results in centennial, multi-stemmed and highly inter-connected individuals with a cooperative behavior that would favor clonal resilience, but that would hinder attempts to high forest conversion.

Acknowledgements

We are grateful to Javier Donés, director of the Centro de Montes y Aserradero de Valsaín, for economic and logistic support. We thank Manuel Iglesias for Figure 6 and his inestimable

494 support in the field and lab work together with César Otero, Guillermo González, Eva Miranda,
495 Paula Guzman, Alfredo Cabranes and Andrés Sanz. We also thank to Drs. Fabio Marzaioli and
496 Filippo Terrasi of the Center for Isotopic Research on the Cultural and Environmental Heritage
497 for radiocarbon dating. Roberto Salomón was supported by a Ph.D. scholarship from the
498 Universidad Politécnica de Madrid. César Morales-Molino holds a Swiss Government Excellent
499 Postdoctoral Scholarship for Foreign Researchers (Ref.: 2014.0386). This work was funded by
500 the CAM P2009/AMB-1668 and P2013/MAE-2760 projects and the Transnational Access to
501 Research Infrastructures activity in the Seventh Framework Programme of the European Union
502 under the Trees4Future project (284181).

503 **References**

504 Ally, D., Ritland, K., Otto, S.P., 2010. Aging in a long-lived clonal tree. PLoS Biol. 8,
505 e1000454. doi:10.1371/journal.pbio.1000454

506 Barbaroux, C., Bréda, N., 2002. Contrasting distribution and seasonal dynamics of carbohydrate
507 reserves in stem wood of adult ring-porous sessile oak and diffuse-porous beech trees.
508 Tree Physiol. 22, 1201–1210. doi:10.1093/treephys/22.17.1201

509 Barbaroux, C., Bréda, N., Dufrêne, E., 2003. Distribution of above-ground and below-ground
510 carbohydrate reserves in adult trees of two contrasting broad-leaved species (*Quercus*
511 *petraea* and *Fagus sylvatica*). New Phytol. 157, 605–615. doi:10.1046/j.1469-
512 8137.2003.00681.x

513 Baret, M., DesRochers, A., 2011. Root connections can trigger physiological responses to
514 defoliation in nondefoliated aspen suckers. Botany 89, 753–761. doi:10.1139/b11-062

515 Bell, T.L., Ojeda, F., 1999. Underground starch storage in *Erica* species of the Cape Floristic
516 Region - differences between seeders and resprouters. New Phytol. 144, 143–152.
517 doi:10.1046/j.1469-8137.1999.00489.x

518 Bell, T.L., Pate, J.S., Dixon, K.W., 1996. Relationships between fire response, morphology, root
519 anatomy and starch distribution in south-west Australian Epacridaceae. Ann. Bot. 77, 357–
520 364. doi:10.1006/anbo.1996.0043

521 Bond, W.J., Midgley, J.J., 2001. Ecology of sprouting in woody plants: the persistence niche.
522 Trends Ecol. Evol. 16, 45–51. doi:10.1016/S0169-5347(00)02033-4

523 Bravo, J.A., Roig, S., Serrada, R., 2008. Selvicultura en montes bajos y medios de *Quercus ilex*
524 L., *Q. pyrenaica* Willd. y *Q. faginea* Lam, in: Serrada, R., Montero, G. (Eds.), Compendio
525 de Selvicultura Aplicada En España. Instituto Nacional de Investigación y Tecnnología
526 Agraria y Alimentaria, Madrid, pp. 657–744.

527 Cairns, M.A., Brown, S., Helmer, E.H., Baumgardner, G.A., 1997. Root biomass allocation in

528 the world's upland forests. Oecologia 111, 1–11. doi:10.1007/s004420050201

529 Camisón, Á., Miguel, R., Marcos, J.L., Revilla, J., Tardáguila, M.Á., Hernández, D., Lakicevic,
530 M., Jovellar, L.C., Silla, F., 2015. Regeneration dynamics of *Quercus pyrenaica* Willd. in
531 the Central System (Spain). For. Ecol. Manage. 343, 42–52.
532 doi:10.1016/j.foreco.2015.01.023

533 Canadell, J., Roda, F., 1991. Root biomass of *Quercus ilex* in a montane Mediterranean forest.
534 Can. J. For. Res. 21, 1771–1778. doi:10.1139/x91-245

535 Cañellas, I., Del Río, M., Roig, S., Montero, G., 2004. Growth response to thinning in *Quercus*
536 *pyrenaica* Willd. coppice stands in Spanish central mountain. Ann. For. Sci. 61, 243–250.
537 doi:10.1051/forest:2004017

538 Cañellas, I., San Miguel, A., 2000. Biomass of root and shoot systems of *Quercus coccifera*
539 shrublands in Eastern Spain. Ann. For. Sci. 57, 803–810. doi:10.1051/forest:2000160

540 Capano, M., Marzaioli, F., Sirignano, C., Altieri, S., Lubritto, C., D'Onofrio, A., Terrasi, F.,
541 2010. ^{14}C AMS measurements in tree rings to estimate local fossil CO_2 in Bosco Fontana
542 forest (Mantova, Italy). Nucl. Instruments Methods Phys. Res. Sect. B Beam Interact. with
543 Mater. Atoms 268, 1113–1116. doi:10.1016/j.nimb.2009.10.112

544 Clarke, P., Lawes, M., Midgley, J., Lamont, B., Ojeda, F., Burrows, G., Enright, N., Knox, K.,
545 2013. Resprouting as a key functional trait: how buds, protection and resources drive
546 persistence after fire. New Phytol. 197, 19–35. doi:10.1111/nph.12001

547 Clarke, P.J., Lawes, M.J., Midgley, J.J., 2010. Resprouting as a key functional trait - challenges
548 to developing new organizing principles. New Phytol. doi:10.1111/j.1469-
549 8137.2010.03508.x

550 Corcuera, L., Camarero, J.J., Sisó, S., Gil-Pelegrín, E., 2006. Radial-growth and wood-
551 anatomical changes in overaged *Quercus pyrenaica* coppice stands: functional responses
552 in a new Mediterranean landscape. Trees 20, 91–98. doi:10.1007/s00468-005-0016-4

de Witte, L.C., Stöcklin, J., 2010. Longevity of clonal plants: why it matters and how to measure it. Ann. Bot. 106, 859–870. doi:10.1093/aob/mcq191

DesRochers, A., Lieffers, V.J., 2001a. The coarse-root system of mature *Populus tremuloides* in declining stands in Alberta, Canada. J. Veg. Sci. 12, 355–360. doi:10.2307/3236849

DesRochers, A., Lieffers, V.J., 2001b. Root biomass of regenerating aspen (*Populus tremuloides*) stands of different densities in Alberta. Can. J. For. Res. 31, 1012–1018. doi:10.1139/cjfr-31-6-1012

Dietze, M.C., Sala, A., Carbone, M.S., Czimczik, C.I., Mantooth, J.A., Richardson, A.D., Vargas, R., 2014. Nonstructural carbon in woody plants. Annu. Rev. Plant Biol. 65, 667–687. doi:10.1146/annurev-arplant-050213-040054

Fraser, E.C., Lieffers, V.J., Landhäusser, S.M., 2006. Carbohydrate transfer through root grafts to support shaded trees. Tree Physiol. 26, 1019–1023. doi:10.1093/treephys/26.8.1019

Genet, H., Bréda, N., Dufrêne, E., 2010. Age-related variation in carbon allocation at tree and stand scales in beech (*Fagus sylvatica* L.) and sessile oak (*Quercus petraea* (Matt.) Liebl.) using a chronosequence approach. Tree Physiol. 30, 177–192. doi:10.1093/treephys/tpp105

Heijari, J., Nerg, A.M., Kainulainen, P., Viiri, H., Vuorinen, M., Holopainen, J.K., 2005. Application of methyl jasmonate reduces growth but increases chemical defence and resistance against *Hylobius abietis* in Scots pine seedlings, in: Entomologia Experimentalis et Applicata. pp. 117–124. doi:10.1111/j.1570-7458.2005.00263.x

Helmisaari, H.-S., Derome, J., Nöjd, P., Kukkola, M., 2007. Fine root biomass in relation to site and stand characteristics in Norway spruce and Scots pine stands. Tree Physiol. 27, 1493–1504. doi:10.1093/treephys/27.10.1493

Hua, Q., Barbetti, M., Rakowski, A.Z., 2013. Atmospheric radiocarbon for the period 1950-2010. Radiocarbon 55, 2059–2072. doi:10.2458/azu_js_rc.v55i2.16177

578 Iwasa, Y., Kubo, T., 1997. Optimal size of storage for recovery after unpredictable disturbances.
579 Evol. Ecol. 11, 41–65. doi:10.1023/A:1018483429029

580 Jelínková, H., Tremblay, F., DesRochers, A., 2009. Molecular and dendrochronological analysis
581 of natural root grafting in *Populus tremuloides* (Salicaceae). Am. J. Bot. 96, 1500–1505.
582 doi:10.3732/ajb.0800177

583 Knox, K.J.E., Clarke, P.J., 2005. Nutrient availability induces contrasting allocation and starch
584 formation in resprouting and obligate seeding shrubs. Funct. Ecol. 19, 690–698.
585 doi:10.1111/j.1365-2435.2005.01006.x

586 Li, M.H., Xiao, W.F., Shi, P., Wang, S.G., Zhong, Y.-D., Liu, X.L., Wang, X.D., Cai, X.H., Shi,
587 Z.M., 2008. Nitrogen and carbon source-sink relationships in trees at the Himalayan
588 treelines compared with lower elevations. Plant, Cell Environ. 31, 1377–1387.
589 doi:10.1111/j.1365-3040.2008.01848.x

590 Manuel Valdés, C., Rojo y Alboreca, A., 1993. Valsaín forest in the XVIII century: an example
591 of forest management in the pre-industrial era. Investig. Agrar. Sist. y Recur. For. 3, 217–
592 229.

593 Millikin, C.S., Bledsoe, C.S., Tecklin, J., 1997. Woody root biomass of 40- to 90- year-old blue
594 oaks (*Quercus douglasii*) in western Sierra Nevada foothills, in: Pillsbury, N.H., Verner,
595 J., Tietje, W.D. (Eds.), Proceedings of a Symposium on Oak Woodlands: Ecology,
596 Management, and Urban Interface Issues. United States Forest Service. Department of
597 Agriculture, Albany, CA, pp. 83–90.

598 Mokany, K., Raison, R.J., Prokushkin, A.S., 2006. Critical analysis of root:shoot ratios in
599 terrestrial biomes. Glob. Chang. Biol. 12, 84–96. doi:10.1111/j.1365-2486.2005.001043.x

600 Montero, G., Ruiz-Peinado, R., Muñoz, M., 2005. Producción de biomasa y fijación de CO_2 por
601 los bosques españoles. Instituto Nacional de Investigación y Tecnología Agraria y
602 Alimentaria, Madrid.

603 Oleksyn, J., Zytkowiak, R., Karolewski, P., Reich, P.B., Tjoelker, M.G., 2000. Genetic and
604 environmental control of seasonal carbohydrate dynamics in trees of diverse *Pinus*
605 *sylvestris* populations. Tree Physiol. 20, 837–847. doi:10.1093/treephys/20.12.837

606 Paula, S., Ojeda, F., 2009. Belowground starch consumption after recurrent severe disturbance
607 in three resprouter species of the genus *Erica*. Botany 87, 253–259. doi:10.1139/B08-134

608 Poorter, H., Niklas, K.J., Reich, P.B., Oleksyn, J., Poot, P., Mommer, L., 2012. Biomass
609 allocation to leaves, stems and roots: meta-analysis of interspecific variation and
610 environmental control. New Phytol. 193, 30–50. doi:10.1111/j.1469-8137.2011.03952.x

611 Poorter, L., Kitajima, K., 2007. Carbohydrate storage and light requirements of tropical moist
612 and dry forest tree species. Ecology 88, 1000–1011. doi:http://dx.doi.org/10.1890/06-0984

613 Reimer, P.J., Bard, E., Bayliss, A., Beck, J.W., Blackwell, P.G., Bronk Ramsey, C., Buck, C.E.,
614 Cheng, H., Edwards, R.L., Friedrich, M., Grootes, P.M., Guilderson, T.P., Haflidason, H.,
615 Hajdas, I., Hatté, C., Heaton, T.J., Hoffmann, D.L., Hogg, A.G., Hughen, K.A., Kaiser,
616 K.F., Kromer, B., Manning, S.W., Niu, M., Reimer, R.W., Richards, D.A., Scott, E.M.,
617 Southon, J.R., Staff, R.A., Turney, C.S.M., van der Plicht, J., 2013. IntCal13 and
618 Marine13 radiocarbon age calibration curves 0–50,000 years cal BP. Radiocarbon 55,
619 1869–1887. doi:10.2458/azu_js_rc.55.16947

620 Reimer, R., Reimer, P.J., 2004. CALIBomb - calibration of post-bomb C-14 data.

621 Robinson, D., 2004. Scaling the depths: below-ground allocation in plants, forests and biomes.
622 Funct. Ecol. 18, 290–295. doi:10.1111/j.0269-8463.2004.00849.x

623 Rodríguez-Calcerrada, J., López, R., Salomón, R., Gordaliza, G., Valbuena-Carabaña, M.,
624 Oleksyn, J., Gil, L., 2015. Stem CO_2 efflux in six co-occurring tree species: underlying
625 factors and ecological implications. Plant, Cell Environ. 38, 1104–1115.
626 doi:10.1111/pce.12463

627 Ruiz-Peinado, R., Montero, G., del Rio, M., 2012. Biomass models to estimate carbon stocks

for hardwood tree species. For. Syst. 21, 42–52. doi:http://dx.doi.org/10.5424/fs/2112211-02193

Sala, A., Woodruff, D.R., Meinzer, F.C., 2012. Carbon dynamics in trees: feast or famine? Tree Physiol. 32, 764–775. doi:10.1093/treephys/tpr143

Salomón, R., Valbuena-Carabaña, M., Gil, L., González-Doncel, I., 2013. Clonal structure influences stem growth in *Quercus pyrenaica* Willd. coppices: Bigger is less vigorous. For. Ecol. Manage. 296, 108–118. doi:10.1016/j.foreco.2013.02.011

Salomón, R., Valbuena-Carbaña, M., Rodríguez-Calcerrada, J., Aubrey, D., McGuire, M., Teskey, R., Gil, L., González-Doncel, I., 2015. Xylem and soil CO_2 fluxes in a *Quercus pyrenaica* Willd. coppice: root respiration increases with clonal size. Ann. For. Sci. 72, 1065–1078. doi:10.1007/s13595-015-0504-7

Serrada Hierro, R., Bravo-Fernández, J.A., Otero de Irizar, J., Ruiz-Peinado Gertrudix, R., Mutke Regneri, S., Roig Gómez, S., 2013. El bosque invisible bajo el monte bajo: una mirada al sistema radical de las cepas de encina, in: Sociedad Española de Ciencias Forestales (Ed.), VI Congreso Forestal Español. Vitoria, pp. 6CFE01–176.

Serrada, R., Allué, M., San Miguel, A., 1992. The coppice system in Spain. Current situation, state of art and major areas to be investigated. Ann. dell´Istituto Sper. del la Selvic. 23, 266–275.

Tandoh, J.B., Marzaioli, F., Battipaglia, G., Capano, M., Castaldi, S., Lasserre, B., Marchetti, M., Passariello, I., Terrasi, F., Valentini, R., 2013. Biomass growth rate of trees from Cameroon based on ^{14}C analysis and growth models. Radiocarbon 55, 885–893. doi:10.2458/azu_js_rc.55.16243

Tanentzap, A.J., Mountford, E.P., Cooke, A.S., Coomes, D.A., 2012. The more stems the merrier: advantages of multi-stemmed architecture for the demography of understorey trees in a temperate broadleaf woodland. J. Ecol. 100, 171–183. doi:10.1111/j.1365-2745.2011.01879.x

654 Tarroux, E., DesRochers, A., 2011. Effect of natural root grafting on growth response of jack
655 pine (*Pinus banksiana*; Pinaceae). Am. J. Bot. 98, 967–974. doi:10.3732/ajb.1000261

656 Tarroux, E., DesRochers, A., Krause, C., 2010. Effect of natural root grafting on growth
657 response of jack pine (*Pinus banksiana*) after commercial thinning. For. Ecol. Manage.
658 260, 526–535. doi:10.1016/j.foreco.2010.05.008

659 Tarroux, E., DesRochers, A., Tremblay, F., 2014. Molecular analysis of natural root grafting in
660 jack pine (*Pinus banksiana*) trees: how does genetic proximity influence anastomosis
661 occurrence? Tree Genet. Genomes 10, 667–677. doi:10.1007/s11295-014-0712-6

662 Valbuena-Carabaña, M., Gil, L., 2013. Genetic resilience in a historically profited root
663 sprouting oak (*Quercus pyrenaica* Willd.) at its southern boundary. Tree Genet. Genomes
664 9, 1129–1142. doi:10.1007/s11295-013-0614-z

665 Valbuena-Carabaña, M., González-Martínez, S.C., Gil, L., 2008. Coppice forests and genetic
666 diversity: A case study in *Quercus pyrenaica* Willd. from Central Spain. For. Ecol.
667 Manage. 254, 225–232. doi:10.1016/j.foreco.2007.08.001

668 Vanninen, P., Makela, A., 1999. Fine root biomass of Scots pine stands differing in age and soil
669 fertility in southern Finland. Tree Physiol. 19, 823–830. doi:10.1093/treephys/19.12.823

670 Ximénez de Embún, J., 1961. El monte bajo. Ministerio de Agicultura, Madrid.

671 Zeppel, M.J.B., Harrison, S.P., Adams, H.D., Kelley, D.I., Li, G., Tissue, D.T., Dawson, T.E.,
672 Fensham, R., Medlyn, B.E., Palmer, A., West, A.G., McDowell, N.G., 2015. Drought and
673 resprouting plants. New Phytol. 206, 583–589. doi:10.1111/nph.13205

674 Zhu, W.-Z., Cao, M., Wang, S.-G., Xiao, W.-F., Li, M.-H., 2012a. Seasonal dynamics of mobile
675 carbon supply in *Quercus aquifolioides* at the upper elevational limit. PLoS One 7,
676 e34213. doi:10.1371/journal.pone.0034213

677 Zhu, W.-Z., Xiang, J.-S., Wang, S.-G., Li, M.-H., 2012b. Resprouting ability and mobile
678 carbohydrate reserves in an oak shrubland decline with increasing elevation on the eastern

679 edge of the Qinghai–Tibet Plateau. For. Ecol. Manage. 278, 118–126.
680 doi:10.1016/j.foreco.2012.04.032
681

682 **Table 1** Aboveground features and dry biomass partitioning of 12 measured stems belonging to
683 two different clones of *Quercus pyrenaica*. Aboveground biomass was separated by
684 organs (stem, branches and leaves); and woody biomass (stem and branches) was
685 separated by tissue (heartwood, sapwood and bark).

Clone	dbh[a] (cm)	Height (m)	Annual growth rings[b]	Biomass (kg)				Woody biomass (kg)		
				Stem	Branches	Leaves	Total	Heartwood	Sapwood	Bark
	15.75	12.67	48	100.8	31.0	4.8	136.6	33.53	63.50	34.79
	21.75	13.75	50	171.6	95.5	8.6	275.7	72.50	124.12	70.42
	20.38	11.65	44	137.8	105.6	8.4	251.8	64.79	115.27	63.38
LARGE	21.50	13.46	46	151.8	69.2	7.0	228	58.25	103.19	59.57
(81 m^2)	17.00	12.51	47	112.5	23.7	3.5	139.7	37.04	65.39	33.77
	22.60	13.27	46	191.5	102.7	10.0	304.2	82.45	134.35	77.38
	12.40	10.97	43	55.3	8.1	2.2	65.6	19.75	26.06	17.65
	11.75	9.94	42	41.4	5.7	1.8	48.9	10.32	23.10	13.63
	21.28	10.46	45	125.1	43.0	5.8	173.9	47.77	80.45	39.92
SMALL	19.30	9.78	48	106.1	22.0	3.5	131.6	35.47	59.80	33.73
(16 m^2)	19.18	9.89	44	95.8	33.3	4.4	133.5	39.32	57.53	31.18
	20.05	9.42	47	100.3	43.9	5.6	149.8	41.68	64.73	37.76

686 [a] dbh: diameter at breast height

687 [b] Annual growth rings counted at breast height at the end of 2013 growing season

688

689 **Table 2** Belowground biomass in two clones of *Quercus pyrenaica* measured after hydraulic
690 excavations. Belowground biomass was separated by root type (taproots, coarse root and fine
691 roots); and woody biomass was separated by tissue (heartwood, sapwood and bark). Fine roots
692 were measured by extracting 24 soil cores and classified by their root diameter.

Root type	Tissue	Clone LARGE (81 m^2)	Clone SMALL (16 m^2)
Taproots biomass (kg)	Heartwood	166.8	31.5
	Sapwood	178.6	35.4
	Bark	66.7	8.5
Coarse roots biomass (kg)	Heartwood	127.1	32.0
	Sapwood	477.1	120.3
	Bark	249.6	62.9
Fine roots (g dm^{-3})	Large fine roots (2-5 mm)	0.29 (0.09)	0.37 (0.11)
	Small fine roots (<2 mm)	3.27 (0.71)	1.43 (0.54)

693

694

695 **Table 3** Root connections within two *Q.pyrenaica* clones of contrasted size observed after
696 hydraulic excavation. The larger clone covered 81 m^2 and was composed by 12 young and 62
697 old taproots. The smaller clone covered 16 m^2 and was composed by four young and two old
698 taproots.

Clone	Connection type	Number	Mean (SE) root diameter[a] (cm)	Σ total section[b] (dm^2)	Σ sapwood section[c] (dm^2)
LARGE (81 m^2)	Graft	189	2.05 (0.07)	7.75	4.8
	Parental root	59	4.42 (0.31)	11.68	6.68
SMALL (16 m^2)	Graft	20	2.59 (0.42)	1.58	0.93
	Parental root	6	14.78 (6.52)	20.32	6.36

699 [a] Diameter of the smallest grafted root was considered for root grafts, and diameter at the
700 midpoint between connected taproots was considered for parental roots.

701 [b] Cumulative total section was the sum of sections at the diameter measuring point of grafts and
702 connecting parental roots considering bark, sapwood and heartwood

703 [c] Cumulative total section was the sum of sections of grafts and connecting parental roots
704 considering uniquely sapwood, estimated from Figure S1 (Relative sapwood section = - 0.02 ×
705 root radius + 0.65).

706

707 **Table 4** Radiocarbon dates of wood samples from the roots of the two clones.

Clone	Sample name	Radiocarbon age (^{14}C yr BP)	Calibrated age, 95.4% confidence interval (cal yr BP)[a]	Estimated age, median (cal yr BP)
LARGE (81 m^2)	VAL-4	70 ± 68	1685 – 1732 AD (21.8%) 1807 – 1928 AD (66.7%) 1955 – 1958 AD (11.6%)	1860 AD
	VAL-3	450 ± 50	1331 – 1338 AD (0.6%) 1397 – 1523 AD (87.1%) 1559 – 1564 AD (0.4%) 1570 – 1631 AD (11.9%)	1450 AD
	VAL-2	53 ± 45	1683 – 1736 AD (26.5%) 1805 – 1934 AD (73.1%) 1955 AD (0.4%)	1850 AD
SMALL (16 m^2)	VAL-1	198 ± 35	1644 – 1694 AD (25.7%) 1726 – 1813 AD (52.4%) 1838 – 1842 AD (0.4%) 1853 – 1867 AD (1.2%) 1918 – 1955 AD (20.3%)	1770 AD

708

709

Figure 1 Biomass partitioning in two clones of *Quercus pyrenaica* of contrasted size, displayed by (a) plant organ (leaves, branches, stems, taproots, coarse roots and fine roots) and (b) plant tissue (heartwood, sapwood and bark) excluding leaves and fine roots. Sapwood non-structural carbohydrate (NSC) pools of the clones (c), calculated as the product of NSC concentration on a dry matter basis by its corresponding sapwood dry biomass. The larger clone was composed by eight stems and it had a clonal extension of 81 m^2, whereas the smaller clone was composed by four stems and it had a clonal extension of 16 m^2.

Figure 2 Relative volume of heartwood, sapwood and bark (on a percentage basis) of taproots originated from stems harvested at three different dates. Young taproots corresponded to stems felled in 2013 (n = 12) and 2008 (n = 4), and old taproots from undated previous cutting (n = 29), most of them exposed after excavation. Different letters indicate significant differences ($P < 0.05$) of relative volumes of tissues among different taproot types. Note the relatively high proportion of functional sapwood in old taproots.

Figure 3 Root-to-shoot ratios of total biomass, woody biomass, sapwood biomass, fine roots to foliage and sapwood NSC pools in two clones of *Quercus pyrenaica* of contrasted size. The horizontal arrows depict the expected R:S ratio of total biomass (0.28) based on a compilation of 31 reports on *Quercus* species (Genet et al., 2010).

Figure 4 Seasonal variations of starch (lower bars), soluble sugars (upper bars) and total non-structural carbohydrates (NSC = soluble sugars + starch) in roots, stems and twigs of seven clones of *Quercus pyrenaica*. Different letters indicate significant differences ($P < 0.05$) in NSC (letters on compiled bars) and starch (letters on lower bars) within organs (lower case letter) and sampling dates (capital letters). Note the highest concentrations in roots in comparison with aboveground organs at any sampling date.

Figure 5 Starch (lower bars), soluble sugars (upper bars) and total non-structural carbohydrates (NSC = soluble sugars + starch) at three sampling dates in roots, stems and twigs of three large (> 45 m^2) and four small (< 20 m^2) clones of *Quercus pyrenaica*. The asterisk indicates significant differences in NSC ($P=0.002$) and starch ($P = 0.004$) between clonal sizes for roots at the dormant period.

Figure 6 Aerial view of the root system of a hydraulically excavated clone of *Quercus pyrenaica*. The clonal root system covered 81 m^2 and was composed by 74 taproots: eight young taproots belonging to felled trees in 2013 (in red), four young taproots of felled trees in 2008 (in blue), and old taproots from previous unrecorded cuttings events (in dark grey). 248 root connections were observed among taproots: 189 root grafts (in red, connected roots in white) and 59 parental root connections (in yellow).

Figure 7 Confidence intervals (2σ, 95.4%) for the ages of the radiocarbon-dated taproots, Sample VAL-1 belongs to the clone SMALL (16 m^2) whereas samples VAL-2 to VAL-4 come from the clone LARGE (86 m^2). Black crosses denote the location of the median of the probability distribution of ages.

Figure
Click here to download high resolution image

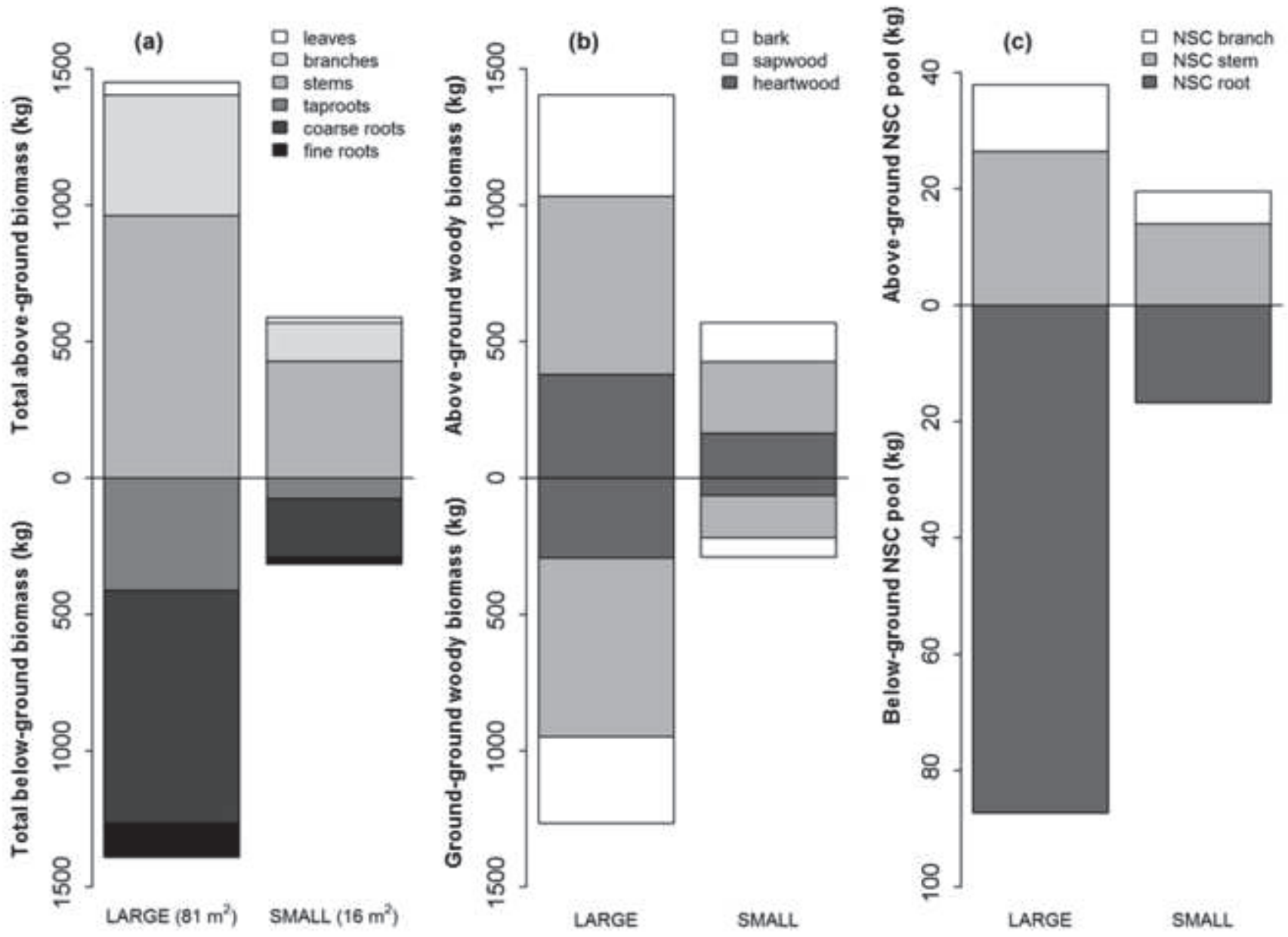

Figure
Click here to download high resolution image

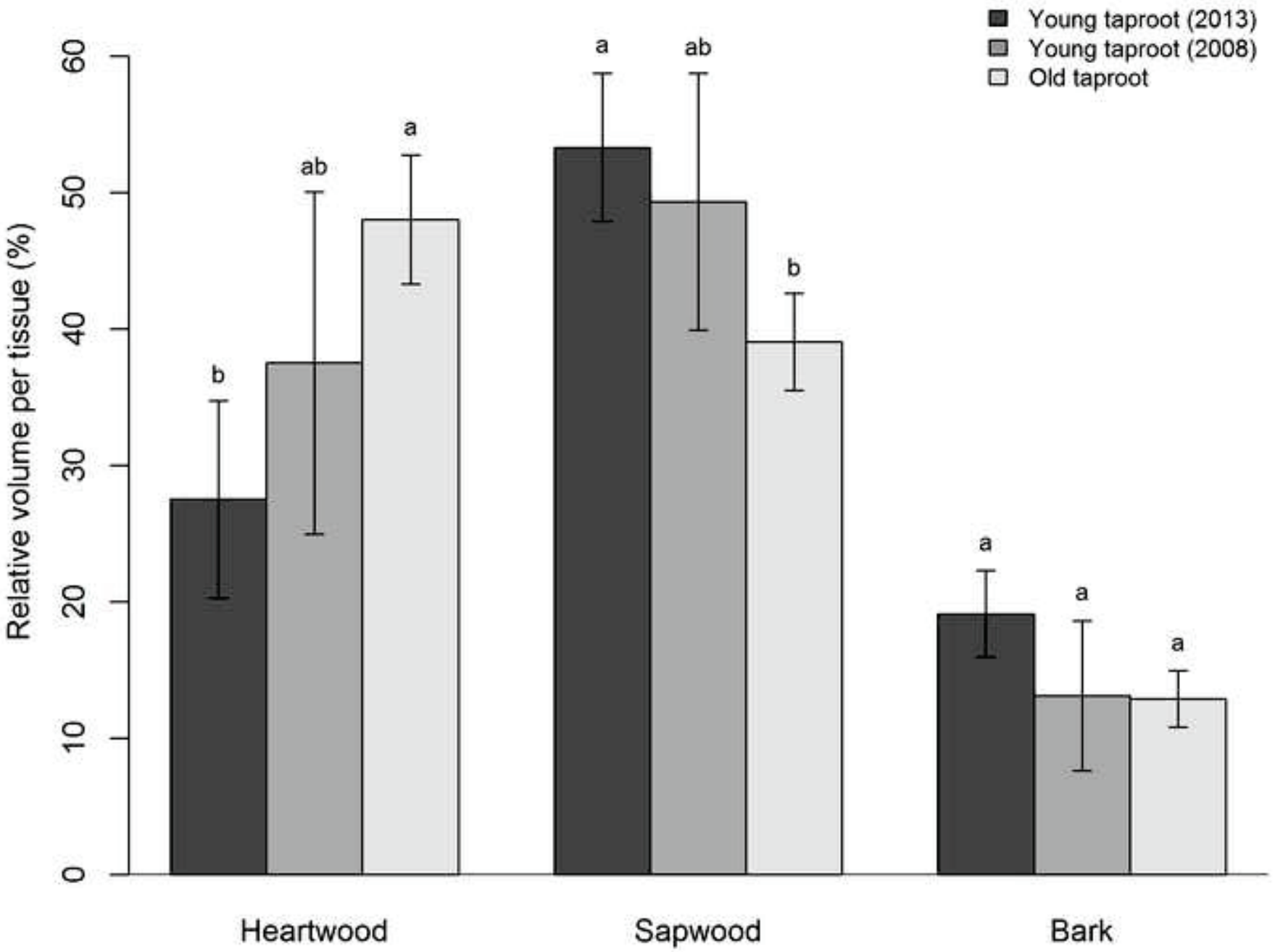

Figure
Click here to download high resolution image

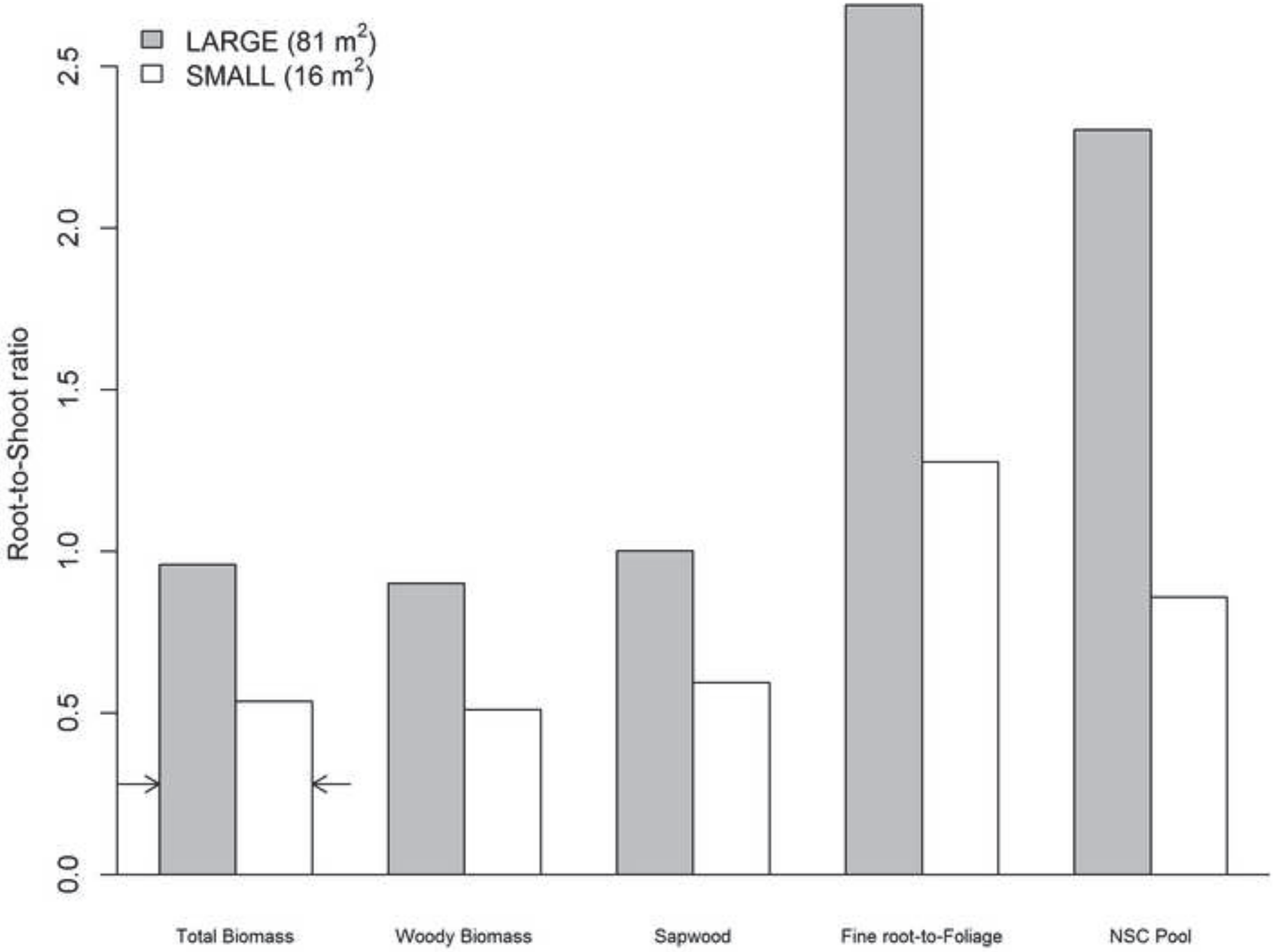

Figure
Click here to download high resolution image

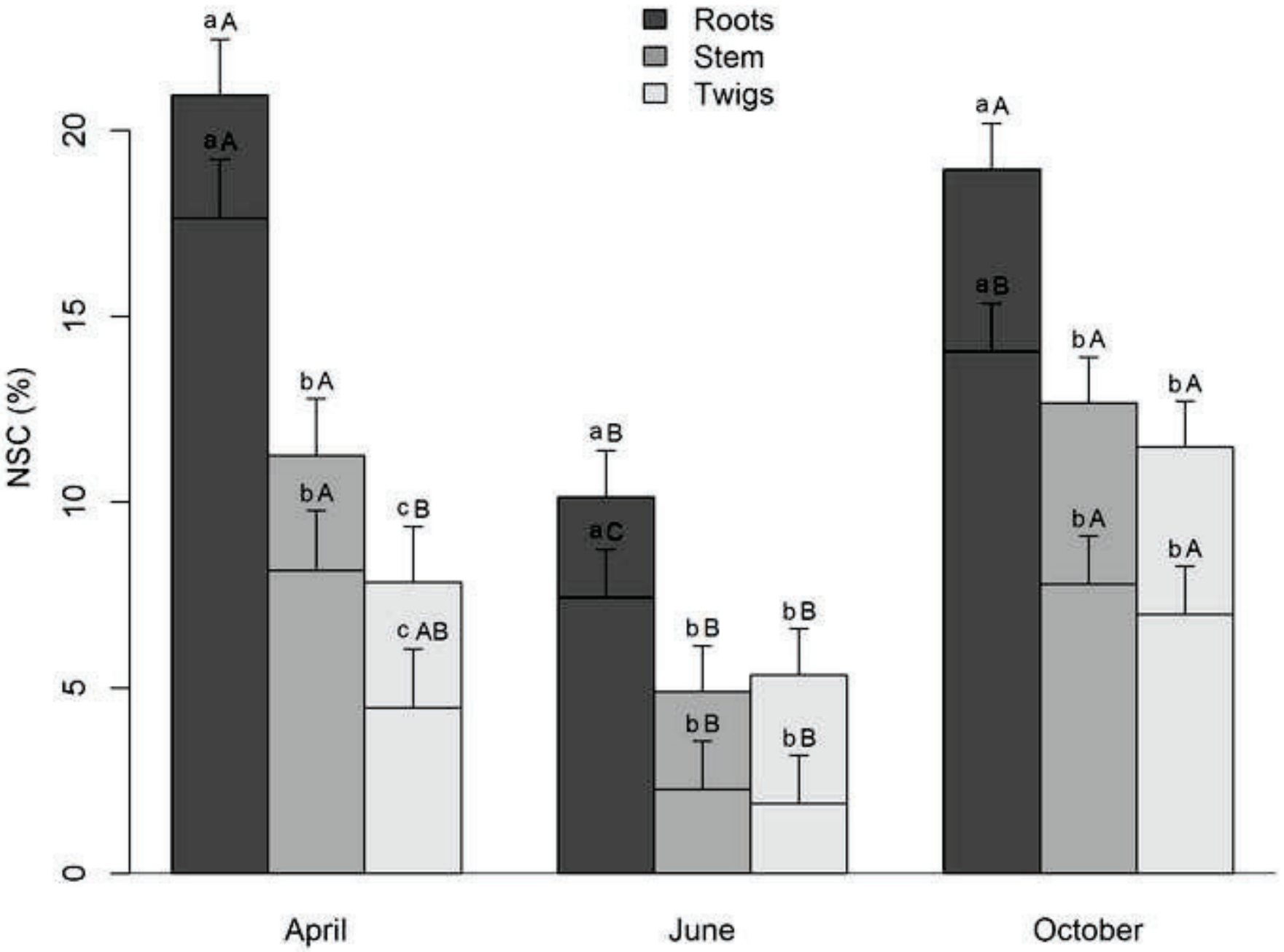

Figure
Click here to download high resolution image

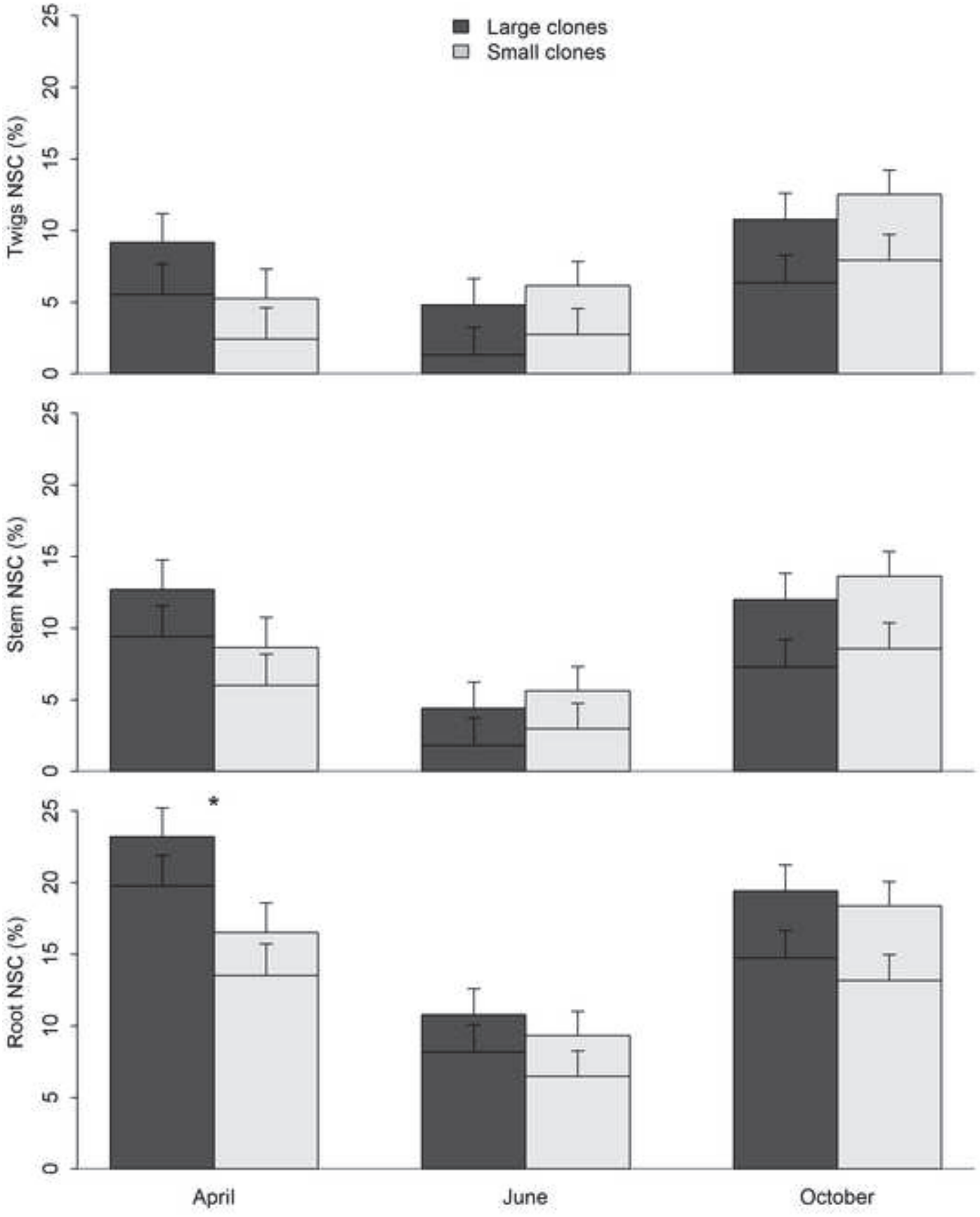

Figure
Click here to download high resolution image

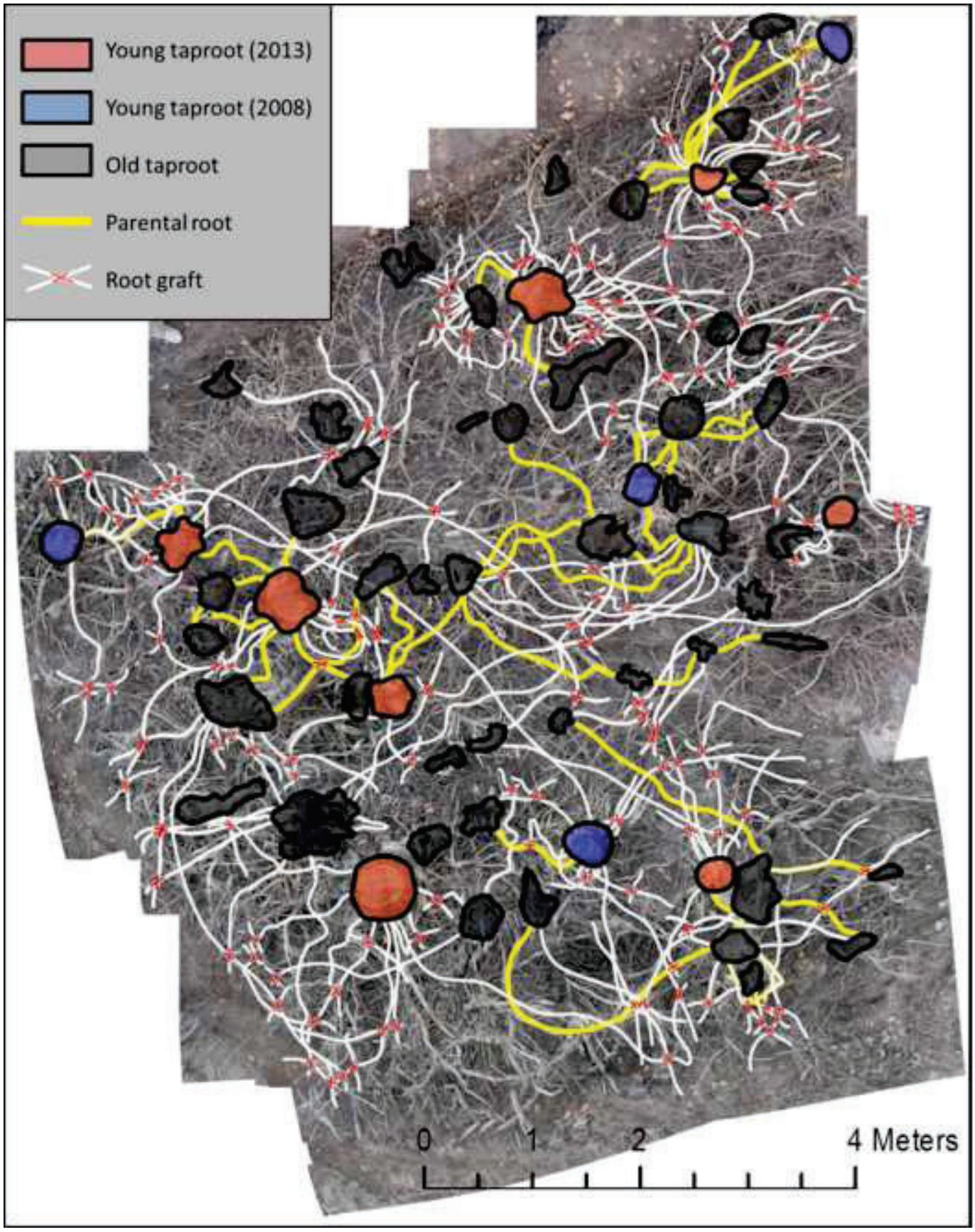

Figure
Click here to download high resolution image